Hydrol. Earth Syst. Sci. Discuss., 10, 12717–12751, 2013
www.hydrol-earth-syst-sci-discuss.net/10/12717/2013/
doi:10.5194/hessd-10-12717-2013

Hydrology and Earth System Sciences Discussions
Open Access

A new technique using the aero-infiltrometer to characterise the natural soils based on the measurements of infiltration rate and soil moisture content

M. A. Fulazzaky[1], **Z. Yusop**[1], **I. Ibrahim**[2], **and A. H. M. Kassim**[2]

[1]Institute of Environmental and Water Resources Management, Water Research Alliance, Universiti Teknologi Malaysia, 81310 UTM Skudai, Johor Bahru, Malaysia
[2]Department of Water and Environment Engineering, Faculty of Civil and Environmental Engineering, Universiti Tun Hussein Onn Malaysia, 86400 Parit Raja, Batu Pahat, Johor, Malaysia

Received: 6 September 2013 – Accepted: 23 September 2013 – Published: 25 October 2013

Correspondence to: M. A. Fulazzaky (fulazzaky@gmail.com)

Published by Copernicus Publications on behalf of the European Geosciences Union.

Abstract

Infiltration rate (f) and soil moisture content (θ) are the important factors for water resources management. Accurate measurements of these factors are not so readily available in most farmlands since present measuring equipments are not really suitable. This paper proposes the measuring device that uses a simple method to measure the rate of water infiltration into the ground and to determine the percentage of water contained in the soil. The two empirical equations which formulated on the basis of power regression models of plotting f vs. air pressure dropping rate (P) and θ vs. P are proposed to evaluate the dynamic properties of soil-water and soil–air interface from a three-phase system. All the parameters in equations have physical meanings, and experimental data validation shows that the equations are sufficiently accurate. Aero-infiltrometer was used to measure both the variations of f and θ at three natural soil sites to contribute to operational water management issues and soil texture identification. In the future, new research opportunities on basic knowledge of air diffusion into the ground will contribute to more versatile techniques in measurement of water infiltration.

1 Introduction

Infiltration as part of hydrologic cycle is the entry of waters into the ground due to gravity forces and initially controlled by capillary forces (Ravi and Williams, 1998), and the hydrologists also remarked it as opposite of seepage. Infiltration is the net movement of water into soil (Davis and Masten, 2004) and has a balance of rainfall from overland flow and evaporation. Rate and quantity of the water which infiltrates into the ground have a function of soil type, soil moisture, soil permeability, land cover, ground surface condition, depth of accumulated water table as well as intensity and volume of precipitation (Wanielista, 1990) and are necessary to be verified for multipurpose land use information. Soil type helps identify size and number of capillaries through

HESSD
10, 12717–12751, 2013

which water and air penetrate a vadose zone. Soil moisture content (θ) helps identify capillary potential and relative conductivity of soil. If the vadose zone has low θ, its capillary potential is high and its conductivity is low (Wanielista, 1990). Soil conductivity to transport a solute increases with θ; heavy rainfall can increase θ (Xu et al., 2012). Depth of groundwater table controls potential amount of water which can infiltrate and potential amount of air which can diffuse from the surface to subsurface land (Peyraube et al., 2012). High groundwater table means that potential infiltration volume is limited. Soil type with its water condition and intensity with volume of precipitation determine amount of water which from precipitation can actually infiltrate into the ground (Wanielista, 1990).

Infiltrometer is a device to be used for measuring rate of water infiltration into the ground and also to determine water content of the soil. The single- or double-ring infiltrometers are commonly used for measuring infiltration rates (f). The others are disc permeameter, tension infiltrometer, turf-tec infiltrometer and sprinkler infiltrometer. There are several challenges related to the use of ring infiltrometers, i.e. (1) pounding of the infiltrometer into the ground deforms the soil, compressing it or causing cracks which can affect the measured infiltration capacity, (2) with a single-ring infiltrometer, water spreads laterally as well as vertically and thus the analysis is more difficult and (3) ring infiltrometers cannot reliably characterise the infiltration of furrow irrigation, of sprinkler irrigation or of rainfall (Bouwer, 1986). In addition, the use of water as dynamic vector is indispensable for measuring rate of water infiltration into the ground when using ring infiltrometers or other classical infiltrometers but it cannot be easily found anywhere. For hydrologists, water engineers, farmers and irrigators, both the measures of f and θ are the important indications concerning the efficiency of irrigation and drainage, optimising the availability of water for plants, improving the yield of crops and minimising erosion (Fulazzaky and Gany, 2009; Wang et al., 2012). The data of f and θ collected especially from a region of high intensity land use are very important for better water management. Unfortunately, the use of such as ring infiltrometer is sometimes difficult due to uncomfortable and unwieldy equipment and is also binding available water. This will be facing the problems of unfitting measurement at slanted lands of the mountain valleys and hilly areas. Still, an alternative measuring device that uses air as dynamic vector has an advantage and is expected to be more versatile techniques. Aero-infiltrometer should be further promoted as an important device for rapid field determination of either f or θ.

A study on two-phase flow equations accounting for air entrapment effects showed that air compression ahead of the wetting front is a major cause of wetting front instability followed by fingering and may affect the change in f significantly (Wang et al., 1997). The mathematical equations derived on the *Green–Ampt* assumptions basis were extended to include the potential effects of air compression and air counter-flow during the water infiltrates into subsurface land (Wang et al., 1997). A model of air-water system by van Genuchten (1980) has already tried to derive a functional correlation between capillary pressure and saturation of the soil and extended by Ippisch et al. (2006), Kutlu and Ersahin (2008), Han et al. (2010), Liu et al. (2011), Valiantzas (2011) and Liu and Xie (2013) in analytical determination of some parameters related to soil science. Still the dynamic and hydraulic circumstances of air diffusion into the ground including the establishment of the correlation plots f vs. air pressure dropping rate (P) or θ vs. P are not fully understood. The objectives of this study are: (1) to propose a new measuring device which is feasible to be used for both the measurements of f and θ, (2) to formulate the empirical equations based on the data of natural soils experiment from the aero-infiltrometer and double-ring infiltrometer and (3) to analyse physical interpretations of the parameters in equations originally reading from the field natural soil experiments supporting with complementary artificial soil data of the laboratory tests for quantitatively characterising the textural features and spatial variability of saturated hydraulic conductivity for different soil types.

2 Methodology

2.1 Design of the aero-infiltrometer and measurement procedure

The components of aero-infiltrometer consist of air tank with 60 cm length and 5 cm diameter, valve, air injection nozzle with a diameter of 2 cm, air input nozzle, and pressure meter, as shown in Fig. 1 (Fulazzaky et al., 2008, 2009a,b). The different diameters of the PVC pipe were designed conical from the air tank to air injection nozzle. The use of PVC pipe to invent the aero-infiltrometer is helpful due to flexible plastic property and low price comparing the other materials of such as glass and steel. The advantages of PVC's aero-infiltrometer are easy to be assembled manually and have the ability to form a sharp edge of air injection nozzle for easily sticking into the ground.

The procedure used to collect the data from an aero-infiltrometer will vary depending on typical design, associated instruments and type of materials. Figure 2 shows the flowchart of aero-infiltrometer test. Notes that: (1) a depth of 6 cm is sufficiently accurate to minimise deformation of soil. The inner wall of air injection nozzle provides like air jacket to diffuse air from the surface to subsurface land. This is analogous to inner tube functioning of a double-ring infiltrometer when water infiltrates and (2) the aims of fitting the 17 psi air pressure are to avoid instability of initial measurement, which can influence the accuracy of the results if air pressure injected is higher than 17 psi, and to maximize the reading of air pressure drop, which probably affects the lack of the results if the pressure is lower than 17 psi.

The spatial variability of saturated hydraulic conductivity in soils has a wide range of several orders of magnitude depending on the soil material (Abdulkadir et al., 2012) and can influence the results. At each location, the measurement of decreasing water level (L_w) using the double-ring infiltrometer was carried out at the same soil type near the measurement of air pressure drop (L_p) using the aero-infiltrometer with a distance of about one meter, and the data obtained from these measurements should be independent of each other. The measurement should be sufficiently reliable and is necessary to be avoided from any risks of such soil deformation which may lead to inaccurate data. For the first time, both the measurements of L_w and L_p at the same time are necessary for calibration and validation of the models. Aero-infiltrometer can then be used solely for the measurements of f and θ if the models have been validated. This offers some advantages because of the experimental practices can reduce deformation and compression of the soil to have wide applications in many types of irrigation system.

2.2 Establishment of the empirical equations

2.2.1 Background

Aero-infiltrometer is feasible to be used for measuring f and θ since the typical equations which correlate contingency of air diffusion to water infiltration into the ground have been established for a natural soil site. In order to establish the empirical models, the following assumptions were made that: (1) water and air are the dynamic vectors, (2) with pressure, air diffuses into the ground and moves from the land surface to subsurface and (3) air movement is analogous to water movement into the ground. Even the circumstances of air-confining vadose zone such as air pressure fluctuation, air eruptions from surface, hysteresis in capillary pressure and macro-porous infiltration affect the rate of water infiltration into the soil (Wang et al., 1997), having a general equation can be useful for determining the variations of f and θ accounting for all these circumstances. The equations to analyse air diffusion into the ground and underground flows have been proposed by Petersen et al. (1994), Bartelt-Hunt and Smith (2002), Althaus et al. (2009) and Aharmouch and Amaziane (2012). Still the application of these equations for natural soils that have heterogeneous structures and erratic particle-size is insufficiently reliable. Dynamic and hydraulic properties of the soil are dependent on the capillary forces and vadose zone components of a three-phase system and thus control air diffusion and water infiltration into the ground. In this study, the empirical equations are able to be formulated considering the most fundamental aspects that both the variations of P and f have the decreasing trends pursuant to time (t).

HESSD
10, 12717–12751, 2013

2.2.2 Data calibration and equations

State of soil can be described considering five soil-forming factors, i.e. parent material, topography, climate, biological activity and time, which can determine soil drainage characteristics. More than 3000 specially named the soil types were recorded (Wanielista, 1990). Simplified approaches to determine f of a soil including the empirical models proposed by Kostiakov (1932) and Horton (1939) use t for the variable. This study used the aero-infiltrometer to monitor L_p and double-ring infiltrometer to monitor L_w pursuant to t. The results of monitoring L_p, L_w and t were used as the data entry in determining the variations of f and θ of the soils. The limitation of this study is the experimental sites conducted on soft clayey soil that influenced the interpretation of the results of more heterogeneous soil types. Data collected from the three natural soil sites around the Universiti Tun Hussein Onn Malaysia campus and supporting by the data of laboratory tests for the artificial sandy clay (50 % sand; 50 % clay) were used to describe the below ground and surface processes that involve the dynamics of air and water movement from the land surface to subsurface.

As starting point to establish the empirical equations that the variable t data (see Table 1) reading from the aero-infiltrometer (Column 1) and double-ring infiltrometer (Column 3) were inserted into one column (Column 5) of cumulative t (Cum.t). The following calibrations (Fig. 3) were made that: (1) both the interpolation and extrapolation can be performed to avoid lack of the cumulative L_p (Cum.$\mathrm{L_p}$) data (Column 6), having the correlation plots the Cum.$\mathrm{L_p}$ vs. Cum.t, and (2) the interpolation can be performed to avoid lack of the cumulative L_w (Cum.$\mathrm{L_w}$) data (Column 7), having the correlation plots Cum.$\mathrm{L_w}$ vs. Cum.t.

By definition, P is the decrease in L_p per unit t, this may be expressed in calculus as:

$$P = \frac{\mathrm{d}L_\mathrm{p}}{\mathrm{d}t} \tag{1}$$

HESSD
10, 12717–12751, 2013

where P is air pressure dropping rate (in psi h^{-1}), dL_p is the change in L_p during dt (in psi), and dt is change of the test time (in h).

One of the oldest and most widely used infiltration equations today was developed by Horton (1939). This equation assumes that rainfall intensity is greater than infiltration capacity at all times and f decreases as t increases (Bedient and Huber, 1992). The Horton equation's major drawback is that it does not consider storage available in the soil after varying amounts of the infiltration have occurred, but only considers infiltration as a function of t (Akan, 1993). In this study, a simplified equation used to determine the experimental f (f_{exp}) is defined as:

$$f_{exp} = \frac{dL_w}{dt} \tag{2}$$

where f_{exp} is experimental infiltration rate (cm h^{-1}), dL_w is the change in L_w during dt (in cm), and dt is change of the test time (in h).

In a stepwise model evaluation strategy, optimum parameters and their sensitivity are identified using calibration and global variance-based sensitivity analysis (Hartmann et al., 2013). The calibration (Column 5) of Cum.t accounting for air diffusion affects to intractable infiltration equation. In keeping with the serial data (see Table 1) of Cum.L_p and Cum.L_w original from field experiments plus inter/extrapolation which have been gathered together (Columns 6–7) were useful for the calculations (Columns 8–9) of P and f_{exp}, respectively. A plot (Fig. 4) of P vs. f_{exp} was rationalised through regression analysis to possess the ability to have a proper formula. The property of equation was selected only the best R^2 from trial amongst the linear, logarithmic, exponential and power regressions. Accordingly, the power regression analysis has a good correlation for all the experiments ($R^2 > 0.907$, see Table 2). This determines the power regression model to represent the data and gives a mathematical expression,

$$f_{th} = \alpha \times P^{\beta} \tag{3}$$

where f_{th} is theoretical infiltration rate (in $cm\,h^{-1}$), P is air pressure dropping rate (in $psi\,h^{-1}$), α is air diffusion coefficient depended on depth of air movement into the ground per unit of pressure (in $cm\,psi^{-1}$), and β is diffusion index depended on size and number of capillaries through which air moves from the surface to subsurface land (dimensionless).

Using Eq. (3) permits us to calculate f_{th} if the parameters α and β as well as the values P were verified for a soil. The infiltration begins at some rates for initial infiltration and exponentially decreases until it reaches a constant rate when soil's porosity is at saturation (Horton, 1939). The variations (Fig. 5) of f_{th} and f_{exp} recorded for each soil site show a similar trend over time. As an example, the f_{th} values calculated using Eq. (3) (Column 10) are close to the f_{exp} values calculated using Eq. (2) (Column 9) for site-1, as shown in Table 1. The empirical equation can be further solved with the natural and pseudo-soil experimentation functions in analysing the dynamic and hydraulic properties of the soil, over this part α indicates the depth of air movement into the ground per unit of pressure and β relates to pore-size distribution and capillary number of the soil through which air flows into the subsurface land. Power regression analysis provides an insight that leads to a better understanding the physical meanings of parameters α and β in Eq. (3).

The movement of water and air in a vadose zone is studied within soil physics and hydrology particularly hydrogeology and is of importance to agriculture, contaminant transport and flood control. Water flows in a vadose zone are often described using the Richard's equation, which partially derived from Darcy's law (Kumar, 2004). Part of the voids in soil is occupied by water and the remainder by air. Rainfall flows through a vadose zone are the primary sources of recharge for aquifer. If the vadose zone envelops soil, the water contained therein is termed soil moisture. Since θ is defined as quantity of the water contained in soil, the portion of the soil volume occupied by water is measured by θ. This property is used to a wide range in scientific and technical areas and is expressed as ratio of the water volume contained in soil, comparing the total volume of vadose zone. The value of θ can range from 0 % when a soil is completely

HESSD
10, 12717–12751, 2013

A new technique using the aero-infiltrometer

M. A. Fulazzaky et al.

dry to 100 % when a soil is fully saturated (van Genuchten, 1980; Dingman, 2002; Lawrence and Hornberger, 2007). In calculus this may be written,

$$\theta_{\text{exp}} = \frac{\Delta \text{Cum.L}_{\text{w}}}{\Delta \text{Cum.L}_{\text{wc}}} \times 100\,\% \tag{4}$$

where θ_{exp} is experimental soil moisture content (in %), ΔCum.L_w is cumulative water infiltration during Δt (in cm), ΔCum.L_{wc} is cumulative water infiltration after achieving at its saturation (in cm).

Having a serial Cum.L_p and Cum.L_w dataset is able using Eq. (1) to calculate P and using Eq. (4) to calculate θ_{exp}. Accordingly, Fig. 6 shows the resulting plots P vs. θ_{exp} and gives the following equation that:

$$\theta_{\text{th}} = \varepsilon \times P^{\gamma} \tag{5}$$

where θ_{th} is theoretically soil moisture content (in %), P is air pressure dropping rate (in psi h^{-1}), ε is soil-air matrix potential coefficient depended on continuous-time to saturate air into the ground per unit of pressure (in % h psi^{-1}), and γ is air-filled porosity index related to capillary potential and relative conductivity (dimensionless).

The use of power regression model ($R^2 > 0.982$, see Table 2) is able to analyse the correlation between θ_{exp} and P. Using Eq. (5) permits to calculate θ_{th} if the parameters ε and γ as well as the values P were verified for a soil. As an example, the θ_{th} values calculated using Eq. (5) (Column 12) are close to the θ_{exp} values calculated using Eq. (4) (Column 11) for site-1, as shown in Table 1. The variations (Fig. 5) of θ_{th} and θ_{exp} pursuant to t show the adjacent trends to recording every site. If the f value decreases toward a constant, the θ value can reach up to 100 % (at its saturation). Water flows into the ground depend on many factors, which can influence the movement of air in a soil, such as void spaces: porosity and resistance and conductive ways: permeability (Wanielista et al., 1997). Physical interpretation of the parameters ε and γ has an intuitive understanding of the time limitation period for air diffusion into the ground and is dependent on capillary potential and continuity of void spaces in soils. The adjacent trends (Fig. 5) in curves f_{th} and f_{exp} as well as in curves θ_{th} and θ_{exp} pursuant to t make a convincing argument that the use of aero-infiltrometer in measuring of f and θ is feasible. Time range of collecting data t and L_p from aero-infiltrometer is faster than that of collecting data t and L_w from double-ring. Still, the extrapolation can be performed to avoid lack of the L_p data since the parameters α, β, ε and γ have been verified for a soil.

3 Discussions

3.1 Typical air pressure dropping rate for the natural soils

It is recognized that P is rate of air diffusion from the surface to subsurface land caused by air pressure and can be calculated using Eq. (1). This study finds (Figs. 4 and 6) that P ranges from 8.6 to 64.3 psi h^{-1}, from 66.9 to 251.4 psi h^{-1} and from 7.2 to 60.1 psi h^{-1} for site-1, site-2 and site-3, respectively (Fulazzaky et al., 2008, 2009a,b). Supposing the variant P is dependent on type and characteristics of the soil. Thus typical P value may typify classification of the soil and is controlled by size, shape and void spaces continuity, which in turn depends on bulk density, structure and texture of the soil. Accordingly, the ability of air movement from the land surface to subsurface is dependent on permeability and capillary potential of the soil.

3.2 Classification of the soils typified by infiltration rate and soil moisture content

Normal non-compacted soils such as grassland have been classified into six textures, i.e. coarse, moderately coarse, medium, moderately fine, fine and very fine (Brady and Weil, 2002). Each classification was named in accordance with the ability of water infiltration into the ground. The following suggestions to classify the type and texture of the soils tested were made based on the literatures by Hillel (1980), Kopec (1995) and Brady and Weil (2002), such that: (1) soil at site-1 typified by f ranging from 4.1 to

$80.6\,\mathrm{cm\,h^{-1}}$ is named as gravel coarse sand and classified into coarse texture, (2) soil at site-2 typified by f ranging from 2.0 to $6.3\,\mathrm{cm\,h^{-1}}$ is named as very fine sandy loam and classified into medium texture and (3) soil at site-3 typified by f ranging from 11.8 to $40.2\,\mathrm{cm\,h^{-1}}$ is named as sand loamy sand and classified into coarse texture. Both the variations (Table 1) of P and f_{exp} show a decreasing trend with increased Cum.t and can consistently correlate with each other. Figure 4 shows the resulting plots P vs. f_{exp} that gives Eq. (3). Correlation for Eq. (3) is good ($R^2 > 0.907$, see Table 2) and hence using Eq. (3) permits us to calculate f_{th}. Figure 5 shows the adjacent curves in the variations of f_{th} andf_{exp} pursuant to t, meaning that air diffusion into the ground can be further proposed for classification of type and texture of the soils. The following suggestions were made based on the results of this study that: (1) coarse textured gravel coarse sand, soil at site-1 that having f ranged from 4.1 to $80.6\,\mathrm{cm\,h^{-1}}$ is typified by P ranging from 8.6 to 64.3 psi $\mathrm{h^{-1}}$, (2) medium textured very fine sandy loam, soil at site-2 that having f ranged from 2.0 to $6.3\,\mathrm{cm\,h^{-1}}$ is typified by P ranging from 66.9 to 251.4 psi $\mathrm{h^{-1}}$ and (3) coarse textured sand loamy sand, soil at site-3 that having f ranged from 11.8 to $40.2\,\mathrm{cm\,h^{-1}}$ is typified by P ranging from 7.2 to 60.1 psi $\mathrm{h^{-1}}$. Both the variations of P and f with t are dependent on pore-size distribution and capillary number of the soil. Physical interpretation for parameters α and β in Eq. (3) can be analysed considering the depth of air movement per unit of pressure and depends on structure and texture of the soil.

Soil specific initial-θ is dependent on spatial-temporal change and controlled by its structure and texture. There are many complexities associated with a vadose zone because of its fissured and fractured nature. Figure 5 shows the adjacent curves for the variations of θ_{th} and θ_{exp} with t. To describe the curves meander of the figure, the following suggestions were made: (1) coarse-textured gravel coarse sand, soil at site-1 has θ ranged from 21.8 to 100 %, (2) medium-textured very fine sandy loam, soil at site-2 has θ ranged from 1.0 to 100 % and (3) coarse-textured sand loamy sand, soil at site-3 has θ ranged from 3.5 to 100 %. The data trends (Table 1) show that P decreases but on the contrary, θ_{exp} increases as the Cum.t increases. Figure 6 plots P

vs. θ_{exp} that gives a power model of Eq. (5) to predict θ_{th} based on the data monitored air diffusion into the ground. Correlation for Eq. (5) is a good ($R^2 > 0.982$, see Table 2). In order to analyse the relationship between θ and P, the following suggestions were made: (1) coarse-textured gravel coarse sand, soil at site-1 that having θ ranged from 21.8 to 100 % is typified by P ranging from 64.3 to 8.6 psi h^{-1}, (2) medium-textured very fine sandy loam, soil at site-2 that having θ ranged from 1.0 to 100 % is typified by P ranging from 251.4 to 66.9 psi h^{-1} and (3) coarse-textured sand loamy sand, soil at site-3 that having θ ranged from 3.5 to 100 % is typified by P ranging from 60.1 to 7.2 psi h^{-1}. Physical interpretation for parameters ε and γ in Eq. (5) may be analysed accounting for continuous-time of air movement per unit of pressure, depending on dynamic and hydraulic properties of the soil. We suppose that the decrease in P with increasing of air pressure in vadose zone is dependent both on capillary potential and relative conductivity of the soil. The interpretation for the correlations of f vs. P and that of θ vs. P helps identify dynamic and hydraulic circumstances of the soil and confirm a simple approach to describe the capillary pressure-saturation behaviour of a three-phase system by a combination of the capillary pressure-saturation functions of two-phase system (van Genuchten, 1980).

3.3 Soil characteristics, air diffusion and infiltration rate

Soil type and degree of soil saturation are the major determining factors of infiltration. Soil is made up of an extensive variety of substances, minerals and rocks. The components composing of a vadose zone can be classified into four groups i.e. minerals, organic matter, air and water. The major components of soil are minerals (sand, silt, clay) and organic matter, which can form its specific texture and structure by which control air and water flow through a vadose zone. In this study, parameter α in Eq. (3) helps identify depth of air diffusion into the ground per unit of pressure and is dependent on air pressure as well as physical and hydraulic properties of the soil. Parameter β in Eq. (3) is dependent on pore-size distribution and capillary number of the soil.

HESSD
10, 12717–12751, 2013

Accordingly, each shape of curve $f_{th} = \alpha \times P^{\beta}$ (see Fig. 4) has a specific inclination to differentiate soil families from each other. Both the variants of α and β could be useful in interpretation of the properties of the soil. An analysis of continuous-time gives insights on dynamic and hydraulic properties of the soil that: (1) water infiltration into gravel coarse sand of site-1 is faster than that into sand loamy sand of site-3 and then that into very fine sandy loam of sites-2 and (2) air diffusion into very fine sandy loam of site-2 is faster than that into gravel coarse sand of site-1 and then that into sand loamy sand of site-3. The movements of air and water are dependent on both the texture and structure of the soil. Large continuous pores of textured coarse permit a rapid water movement through the gravel coarse sand of site-1 and sand loamy sand of site-3 due to coarse-textured properties of having a greater surface roughness are advantageous to water movement (Brady and Weil, 2002). Because of the porous medium properties often resulting in abrupt transitions so less permeable very fine sandy loam of sites-2 is more suitable for air movement there is due to the soil characteristics having pore-size distribution and capillary number are less suitable for water movement. Considering that variant α may typify the depth of air movement into the ground per unit of air pressure. This study finds that air diffusion into sand loamy sand of site-3 is deeper than that into gravel coarse sand of site-1 and then that into very fine sandy loam of site-2, judging the decrease in α value from 4.3 to 0.2 and to 0.1 $\text{cm}\,\text{psi}^{-1}$ was verified for site-3, site-1 and site-2, respectively (see Table 3). Air pressure within a very fine sandy loam is low because of air conjunction from the atmosphere is difficult. Air can move easily from the region of high energy in the air tank to low energy in subsurface land because the gradient of potential energy is high. As a consequence, air movement into a medium-textured soil is fast enough for air penetration. Air diffusion into the ground is controlled by capillary forces consisting of pore-size distribution and number of capillaries. Even the f model (Fig. 7) looks like the Horton's equation, indicating that f decreases with t. Still the trend in curve $f_{th} = \alpha \times P^{\beta}$ modelling for the three soil sites (see Fig. 4) is different from each other. Gravel coarse sand (site-1) has typical characteristics of pore-size distribution and capillary number and is more suitable for both

HESSD
10, 12717–12751, 2013

the movements of water and air, judging by a 1.5 β value is quite important comparing with very fine sandy loam having a 0.8 β value (site-2) and sand loamy sand having a 0.5 β value (site-3), as shown in Table 3.

The interpretation of parameters $\alpha$and β in Eq. (3) associated with air diffusion into the ground might be highly problematic. It is necessary to perform a confirmatory experiment to verify the results from the natural soil tests. This considers physical interpretation of the mathematical theory of air diffusion by pressure to be easier fitting the parameters in modelling efforts. For example, Millington's relation works well to predict the effective diffusion coefficients in homogeneous soils with relatively uniform particle-size distributions (Bartelt-Hunt and Smith, 2002). Based on the laboratory test data of using the artificial sandy clay this study found that α value can significantly increase with increasing of the initial-θ, as shown in Table 4. Under moist air diffusion rate decreases because of the water in vadose zone probably deforms the soil, compressing it or causing cracks (Bouwer, 1986). Its water content makes the soils change dimensions at impregnation and surface roughness degraded to impede air movement. The following suggestions may help identify the properties of the soil that: (1) physical interpretation of parameter α relates to permeability of the soil to diffuse air. Supposing that permeability of the soil decreases as the initial-θ increases and thus an increase in α value can be verified based on the laboratory tests. The results confirm that the increase in α value from 3.0 to 3.5 and to 5.8 $\mathrm{cm\,psi^{-1}}$ is due to the initial-θ increases from 10 to 15 and to 25 %, respectively and (2) physical interpretation of parameter β relates to pore-size distribution and capillary number of the soil. Potential of air diffusion into the subsurface can decrease with increasing of the initial-θ of the soil and thus parameter β can be used as indicator of air movement. The results confirm that the decrease in β value from 0.6 to 0.6 and to 0.4 is due to the initial-θ increases from 10 to 15 and to 25 %, respectively (see Table 4).

Dry condition of soil can provide high capillary potential and is quite suitable for air and water movement. Air diffusion rate decreases as initial-θ increases. Pore-size distribution and capillary number of the soil effect on air diffusion into the ground. Porosity

HESSD
10, 12717–12751, 2013

and pore-size distribution of the soil governs its permeation and can be described in terms of β value. Soil particles when adsorb water reduce its capillary potential to diffuse air. Dry soil is a condition for better pore-size distribution and initial capillary number and has a greater hydraulic gradient provided by high capillary potential. Water seeping into capillaries of the soil can change soil texture conditionally and makes impediment of air movement. As a consequence, air diffusion into the ground decreases with increasing of the water content. The application of Eq. (3) for measuring f depends on the verification of parameters α and β of the soils. Therefore, the future research opportunities need to be addressed as priority the study of air diffusion from the surface to subsurface land.

3.4 Moisture characteristics, air diffusion and soil moisture content

The interpretation of parameter ε in Eq. (5) associated with continuous-time of air diffusion into the ground per unit of air pressure might be dependent on permeability of the soil to diffuse air. Capillary potential and relative conductivity in soil can be identified in terms of γ value. Parameters ε and γ in Eq. (5) can be useful for determining the moisture characteristics of soil due to soil moisture trends of the natural soils can be differentiated from one another by either the parameters ε or γ. The results (Fig. 8) show that application of the different P range can differentiate t to saturate air into the ground, depending on nature and properties of the soils. The fluidity and other dynamic physical properties of soil depend on air–water–soil interface. The figure shows that t required to saturate air into medium-textured soil of very fine sandy loam (site-2) is faster than that into coarse-textured soil of sand loamy sand (site-3) and then that into coarse-textured soil of gravel coarse sand (site-1). Intrinsic permeability of soil makes different continuous-time to diffuse air from the land surface to subsurface. The soil typified by medium-textured soil of very fine sandy loam is faster than coarse-textured soil of sand loamy sand and of gravel coarse sand to diffuse air from the surface to subsurface land. Experimental data (Table 3) validation shows that a ε value of 9×10^7 % h psi^{-1} higher than that of 2632 % h psi^{-1} and then higher that of 489.6 % h psi^{-1}

HESSD
10, 12717–12751, 2013

for site-2, site-3 and site-1, respectively, was verified. The presence of organic matter in coarse-textured soil of gravel coarse sand (site-1) that having an initial-θ of 21.8 % acts like glue to aggregate individual soil particles together to impede air movement. The aggregation is quite difficult for coarse-textured soil of sand loamy sand with an initial-θ of 3.5 % (site-3) and for medium-textured soil of very fine sandy loam with an initial-θ of 1.0 % (site-2) due to their initial-θ is low. With drier soil conditions in dry season, air diffusion into the ground is rapid enough indicating that ε value is important for permeability of the soil. Continuous-time is short for dry soil because of its permeability to saturate air is high. The θ model (Fig. 8) shows that continuous-time of 10 min for medium-textured soil of very fine sandy loam (site-2) is significantly faster than that of 24 min for coarse-textured soil of sand loamy sand (site-3) and then that of 25 min for coarse-textured soil of gravel coarse sand (site-1).

A theoretic approach for interpretation of air diffusion into the ground considers that water contained in vadose zone has a negative pressure head which is below than the atmospheric pressure (Kresic, 2007). The negative γ value (see Tables 3 and 4) might be related to negative air pressure in soil and would record as a suggestion. Air with an initial pressure of 17 psi can move from the air tank to medium-textured soil of very fine sandy loam faster than that to coarse-textured soil of sand loamy sand and then that to coarse-textured soil of gravel coarse sand. Experimental data (Table 3) validation shows that a γ value of −3.2 lower than that of −1.6 and then that of −0.7 was verified for site-2, site-3 and site-1, respectively. A typical γ value of the soil is dependent on porosity which relies on its capillary potential and relative conductivity. As a consequence, the continuous-time to saturate air from the surface to subsurface land is dependent on the texture and structure of the soil.

In the previous studies by DiGiulio (1992) and Suthersan (1999) have reported that air permeability in soil is a function of the soil's intrinsic permeability and liquid content. In this study, a research question can be made into a hypothesis that air permeability in a soil is good for drier soil conditions of low θ. The change in ε value related to initial-θ was analysed accounting for dynamic properties of soil–air interface and requires

HESSD
10, 12717–12751, 2013

Title Page
Abstract Introduction
Conclusions References
Tables Figures
◂◂ ▸▸
◂ ▸
Back Close
Full Screen / Esc
Printer-friendly Version
Interactive Discussion

a quantitative understanding of the process in a vadose-zone. The results (Table 4) of testing the artificial sandy clay validate this hypothesis and show the decrease in ε value from 14,9 to 12,1 to 4,1 % h psi^{-1} with increasing of the initial-θ from 10 to 20 to 25 %, respectively. It is suggested that air diffusion into a dry vadose zone is favourable because of the soil pore space is sufficiently important. Air can diffuse rapidly from the land surface to subsurface because of the passage of air particles through the large soil pores distribution has a high concentration gradient (Fulazzaky, 2011; Fulazzaky et al., 2013). Air permeability in the soil decreases with θ there is due to water can seep into the soil to reduce void spaces. The ability of a soil to freely transmit air is favourable for drier soil conditions due to capillary potential and relative conductivity is sufficiently conducive when air pressure in a vadose zone is below than the atmospheric pressure. The results (Table 4) obtained from the laboratory tests for the assessment of artificial sandy clay show that capillary potential and relative conductivity of the soil decrease with increasing of the initial-θ judging the decrease in γ value from -1.4 to -1.6 to -1.7 with increasing of the initial-θ from 10 to 20 to 25 %, respectively. Air permeability in a soil is dependent on air pressure head, pore size distribution and capillary number. Initial differences in structure and porosity as reported by Foley et al. (2006) were transient and related to θ. It has been found (see Table 4) that the decrease in ε value and the increase in γ value with increasing of the initial-θ seem to be a better indicator for describing air permeability in soils. The continuous-time to air and water flow into the ground must be readily accessible to actual condition, starting from any initial-θ up to soil's saturation (θ = 100 %) and is dependent on capillary potential and relative conductivity of the soil.

4 Conclusions

This study used the data of L_p reading from the aero-infiltrometer and L_w from the double-ring infiltrometer to establish the empirical models. The models must be calibrated and validated before they can be used for the measurements of f and θ of the soil. The empirical models were verified using independent datasets from three natural soil sites. Functional infiltration expressions accounting for air pressure and soil porosity in relation with depth of air movement into the ground and characteristics of the soil were presented. Functional soil moisture expressions accounting for air pressure and soil porosity in relation with continuous-time, capillary potential and relative conductivity were presented as well. All the parameters in equations have physical interpretation, and experimental data validation shows that the equations are sufficiently accurate. Aero-infiltrometer using air as dynamic vector has been proposed as a new device for the measurements of f and θ and gives a forum in understanding the dynamic and hydraulic properties of the soil in a vadose zone. The use of aero-infiltrometer to determine f and θ is helpful due to easy and modest equipment is suitable to be used at any places of critical land. The advantages of aero-infiltrometer are that: (1) the use of air as dynamic vector is available anywhere, (2) the time period for data collection is significantly faster comparing that using the traditional infiltrometers, (3) the physical interpretation of circumstances of air-confining vadose zone may be simplified in terms of the parameters in equations and (4) the use of only two parameters i.e. α and β for measuring f as well as ε and γ for measuring θ is simple in calculation and can minimise the possibility of misinterpretation of the data.

Acknowledgements. This study used the financial supports of Short Grant (SG) Vot. No 0562 from Universiti Tun Hussein Onn Malaysia and Academic Visitor Grant (AVG) Vot. No 4D058 from Universiti Teknologi Malaysia. The SG and AVG provided by the universities are greatly appreciated.

References

Abdulkadir, A., Abdu, N., and Jibril, I.: Application of Kozeny-Carman equation to estimate saturated hydraulic conductivity of an alfisol at Samaru and a cambisol at Kadawa, Nigeria, Nig. J. Basic Appl. Sci., 20, 116–124, 2012.

Aharmouch, A., and Amaziane, B.: Development and evaluation of a numerical model for steady state interface and/or free surface groundwater flow, J. Hydrol., 434–435, 110–120, doi:10.1016/j.jhydrol.2012.02.027, 2012.

Akan, A. O.: Urban Stromwater Hydrology: A Guide to Engineering Calculations, Technomic Publishing Co. Inc., Lancaster, 1993.

Althaus, R., Klump, S., Onnis, A., Kipfer, R., Purtschert, R., Stauffer, F., and Kinzelbach, W.: Noble gas tracers for characterisation of flow dynamics and origin of groundwater: a case study in Switzerland, J. Hydrol., 370, 64–72, doi:10.1016/j.jhydrol.2009.02.053, 2009.

Bartelt-Hunt, S. L. and Smith, J. A.: Measurement of effective air diffusion coefficients for trichloroethene in undisturbed soil cores, J. Contam. Hydrol., 56, 193–208, doi:10.1016/S0169-7722(01)00209-1, 2002.

Bedient, P. B. and Huber, W. C.: Hydrology and Floodplain Analysis, Addison Wesley Publishing Co., New York, 1992.

Bouwer, H.: Intake rate: Cylindrical infiltrometer, in: Methods of Soil Analysis, 2nd Edn., edited by: Klute, A., Soil Science Society of America, Madison, Wisconsin, 825–843, 1986.

Brady, N. C. and Weil, R. R.: The Nature and Properties of Soils, 13th Edn. Prentice-Hall Inc. Upper Saddle River, New Jersey, 2002.

Davis, L. D. and Masten, S. J.: Principles of Environmental Engineering and Science, Mc Graw Hill, Boston, 2004.

Dingman, S. L.: Physical Hydrology, chapter 6: water in soils – infiltration and redistribution, 2nd Edn., Prentice-Hall, Inc. Upper Saddle River, New Jersey, 2002.

Foley, J. L., Tolmie, P. E., and Silburn, D. M.: Improved measurement of conductivity on swelling clay soils using a modified disc permeameter method, Austr. J. Soil Res., 44, 701–710, doi:10.1071/SR05195, 2006.

Fulazzaky, M. A.: Determining the resistance of mass transfer for adsorption of the surfactant onto granular activated carbons from hydrodynamic column, Chem. Eng. J., 166, 832–840, doi:10.1016/j.cej.2010.11.052, 2011.

Fulazzaky, M. A. and Gany, A. H. A.: Challenges of soil erosion and sludge management for sustainable development in Indonesia, J. Environ. Manage., 90, 2387–2392, doi:10.1016/j.jenvman.2009.02.017, 2009.

Fulazzaky, M. A., Kassim, A. H. M., and Ibrahim, I.: Measuring the infiltration rate and soil moisture content by using aero-infiltration tool in order to optimize agricultural water uses, The 20th Congress on Irrigation and Drainage, 13–18 October 2008, Lahore, Pakistan, 2008.

Fulazzaky, M. A., Ismail, I., and Kassim, A. H. M.: Feasibility to use aero-infiltrometer in measuring of the infiltration rate and soil moisture content, International Conference on Water Resources, 26–27 May 2009, Langkawi, Malaysia, 2009a.

Fulazzaky, M. A., Ismail, I., and Kassim, A. H. M.: Empirical models of aero-infiltromater to measure the infiltration rate and soil moisture content, The 3rd Regional Conference on Natural Resources in the Tropics, 2–5 August 2009, Kuching, Malaysia, 2009b.

Fulazzaky, M. A., Khamidun, M. H., and Omar, R.: Understanding of mass transfer resistance for the adsorption of solute onto porous material from the modified mass transfer factor models, Chem. Eng. J., 228, 1023–1029, doi:10.1016/j.cej.2013.05.100, 2013.

Han, X. W., Shao, M. A., and Horton, R.: Estimating van Genuchten model parameters of undisturbed soils using an integral method, Pedosphere, 20, 55–62, doi:10.1016/S1002-0160(09)60282-4, 2010.

Hartmann, A., Weiler, M., Wagener, T., Lange, J., Kralik, M., Humer, F., Mizyed, N., Rimmer, A., Barberá, J. A., Andreo, B., Butscher, C., and Huggenberger, P.: Process-based karst modelling to relate hydrodynamic and hydrochemical characteristics to system properties, Hydrol. Earth Syst. Sci., 17, 3305–3321, doi:10.5194/hess-17-3305-2013, 2013.

Hillel, D.: Fundamentals of Soil Physics. Academic Press, New York, 1980.

Horton, R. E.: An approach toward a physical interpretation of infiltration capacity, Trans. Am. Geophys. Union, 20, 692–711, 1939.

Ippisch, O., Vogel, H. J., and Bastian, P.: Validity limits for the van Genuchten-Mualem model and implications for parameter estimation and numerical simulation, Adv. Water Resour., 29, 1780–1789, doi:10.1016/j.advwatres.2005.12.011, 2006.

Kopec, D. M.: Soil Characteristics and How They Affect Soil Moisture, Turf Tips-Cooperative Extension, Volume II, Issue 10, 1995.

Kostiakov, A. N.: On the dynamic of the coefficient of water percolation in soils and on the necessity of studying it from a dynamic point of view for the purposes of amelioration, in:

Transaction of the 6th Commission of the International Society of Soil Sciences, Moscow, Russia, 1932.

Kresic, N.: Hydrogeology and Groundwater Modeling, 2nd Edn., CRC Press, New York, 2007.

Kumar, P.: Layer averaged Richard's equation with lateral flow, Adv. Water Resour., 27, 521–531, doi:10.1016/j.advwatres.2004.02.007, 2004.

Kutlu, T. and Ersahin, S.: Calibration of van Genuchten unsaturated hydraulic conductivity parameters by regression technique, International Meeting on Soil Fertility, Land Management and Agroclimatology, 29 October–1 November 2008, Kusadasi, Turkey, 175–181, 2008.

Lawrence, J. E. and Hornberger, G. M.: Soil moisture variability across climate zones, Geophys. Res. Lett., 34, L20402, doi:10.1029/2007GL031382, 2007.

Liu, J.-G. and Xie, Z.-H.: Improving simulation of soil moisture in China using a multiple meteorological forcing ensemble approach, Hydrol. Earth Syst. Sci., 17, 3355–3369, doi:10.5194/hess-17-3355-2013, 2013.

Liu, X., Yo, X., and Xu, S.: A new method to estimate the parameters of van Genuchten retention model using degree of phosphorus saturation (DPS), Afr. J. Agric. Res., 6, 4800–4806, doi:10.5897/AJAR11.700, 2011.

Petersen, L. W., Rolston, D. E., Moldrup, P., and Yamaguchi, T.: Volatile organic vapor diffusion and adsorption in soils, J. Environ. Qual., 23, 799–805, 1994.

Peyraube, N., Lastennet, R., and Denis, A.: Geochemical evolution of groundwater in the unsaturated zone of a karstic massif, using the P_{CO_2}-SIc relationship, J. Hydrol., 430–431, 13–24, doi:10.1016/j.jhydrol.2012.01.033, 2012.

Ravi, V. and Williams, J. R.: Estimation of infiltration rate in the vadose zone: compilation of simple mathematical models, Vol. I, EPA/600/R-97-128a, USEPA, Oklahoma, 1998.

Valiantzas, J. D.: Combined Brooks-Corey/Burdine and van Genuchten/Mualem closed-form model for improving prediction of unsaturated conductivity, J. Irrig. Drain. Eng., 137, 223–233, doi:10.1061/(ASCE)IR.1943-4774.0000284, 2011.

van Genuchten, M. T.: A closed-form equation for predicting the hydraulic conductivity of unsaturated soils, Soil Sci. Soc. Am. J., 44, 892–898, 1980.

Wang, G., Jiang, H., Xu, Z., Wang, L., and Yue, W.: Evaluating the effect of land use changes on soil erosion and sediment yield using a grid-based distributed modelling approach, Hydrol. Process., 26, 3579–3592, doi:10.1002/hyp.9193, 2012.

Wang, Z., Feyen, J., Nielsen, D. R., and van Genuchten, M. T.: Two-phase flow infiltration equations accounting for air entrapment effects, Water Resour. Res., 33, 2759–2767, doi:10.1029/97WR01708, 1997.

Wanielista, M.: Hydrology and Water Quantity Control, John Wiley & Sons, Inc., New York, 1990.

Wanielista, M., Kersten, R., and Eaglin, R.: Hydrology – Water Quantity and Water Quality Control, 2nd Edn., John Wiley & Sons, Inc., New York, 1997.

Xu, Q., Liu, S., Wan, X., Jiang, C., Song, X., and Wang, J.: Effects of rainfall on soil moisture and water movement in a subalpine dark coniferous forest in southwestern China, Hydrol. Process., 26, 3800–3809, doi:10.1002/hyp.8400, 2012.

Table 1. An example of the results of aero-infiltrometer and double-ring infiltrometer test collected from site-1.

AI		DRI		Cum.t	Cum.L_p	Cum.L_w	P	f_{exp}	f_{th}	θ_{exp}	θ_{th}
t_{av} (s) (1)	L_p (psi) (2)	t (s) (3)	L_w (cm) (4)	(mn) (5)	(psi) (6)	(cm) (7)	(psi h^{-1}) (8)	(cm h^{-1}) (9)	(cm h^{-1}) (10)	(%) (11)	(%) (12)
0	17.0	0	5.0	0.0	0.0	0.0	64.3	80.6	76.9	21.8	24.7
40	16.5			0.7	0.5	0.5	45.0	47.1	45.5	30.8	31.7
121	16.0			2.0	1.0	0.8	29.8	22.3	24.7	44.1	42.2
294	15.5			4.9	1.5	1.0	18.4	12.3	12.2	58.9	59.0
		300	4.0	5.0	1.5	1.0	18.2	12.0	12.0	58.8	59.3
532	15.0			8.9	2.0	1.2	13.5	8.2	7.8	71.5	72.9
		600	3.7	10.0	2.2	1.3	13.2	7.8	7.5	76.5	74.3
		900	3.6	15.0	2.7	1.4	10.9	5.6	5.6	82.4	84.7
		1200	3.4	20.0	3.2	1.6	9.5	4.8	4.6	94.1	93.0
		1500	3.3	25.0	3.6	1.7	8.6	4.1	4.0	100.0	100.0
		1800	3.3	30.0	3.9	1.7	7.9	3.4	3.5	100.0	
		2100	3.3	35.0	4.3	1.7	7.3	2.9	3.1	100.0	

Notes: AI is Aero-infiltrometer, DRI is double-ring infiltrometer, Cum.L_p is cumulative level of the air pressure drop (in psi), Cum.L_w is cumulative decreasing of the water level (in cm), Cum.t is cumulative test time (in mn), f_{exp} is experimental infiltration rate (cm h^{-1}), f_{th} is theoretical infiltration rate (cm h^{-1}), L_p is level of the air pressure drop (in psi), L_w is decreasing of the water level (in cm), P is air pressure dropping rate (in psi h^{-1}), t is test time (in s), t_{av} is average test time (in s), θ_{exp} is experimental soil moisture content (in %), θ_{th} is theoretical soil moisture content (in %).

HESSD
10, 12717–12751, 2013

A new technique using the aero-infiltrometer

M. A. Fulazzaky et al.

Table 2. Analysis of R^2 from trial of linear, logarithmic, exponential and power regression.

Location of measurement	Correlation coefficient, R^2			
	linear	logarithmic	exponential	power
Trial for infiltration rate correlation				
Site-1	0.9754	0.8452	0.9246	0.9977
Site-2	0.8563	0.9263	0.9252	0.9583
Site-3	0.8646	0.8488	0.7058	0.9077
Trial for soil moisture content correlation				
Site-1	0.8471	0.9685	0.9507	0.9940
Site-2	0.7589	0.8553	0.9608	0.9821
Site-3	0.6629	0.8773	0.9362	0.9965

Note: R^2 is correlation coefficient.

HESSD
10, 12717–12751, 2013

Table 3. Values of α, β, ε and γ for the different sites of natural soil investigation.

Location of investigation	Curve $f_{th} = \alpha \cdot P^{\beta}$			Curve $\theta_{th} = \varepsilon \cdot P^{\gamma}$		
	α (cm psi^{-1})	β	R^2	ε (% h psi^{-1})	γ	R^2
Site-1	0.2	1.5	0.9977	489.6	−0.7	0.9940
Site-2	0.1	0.8	0.9583	9×10^7	−3.2	0.9821
Site-3	4.3	0.5	0.9077	2632	−1.6	0.9965

Notes: f_{th} is theoretical infiltration rate (cm h^{-1}), P is air pressure dropping rate (in psi h^{-1}), R^2 is correlation coefficient (dimensionless), α is air diffusion coefficient relying the depth of air movement into the ground per unit of pressure (in cm psi^{-1}), β is diffusion index relying the size and number of capillaries through which air moves from the surface to subsurface land (dimensionless), ε is soil-air matrix potential coefficient relying the continuous-time to saturate air into the ground per unit of pressure (in % h psi), and γ is air-filled porosity index related to capillary potential and relative conductivity (dimensionless), θ_{th} is theoretical soil moisture content (in %).

HESSD
10, 12717–12751, 2013

HESSD
10, 12717–12751, 2013

A new technique using the aero-infiltrometer

M. A. Fulazzaky et al.

Title Page
Abstract | Introduction
Conclusions | References
Tables | Figures
◀◀ | ▶▶
◀ | ▶
Back | Close
Full Screen / Esc
Printer-friendly Version
Interactive Discussion

Table 4. Values of α, β, ε and γ for artificial sandy clay tested with the different initial-θ.

Initial-θ (%)	Curve $f_{th} = \alpha \times P^{\beta}$			Curve $\theta_{th} = \varepsilon \times P^{\gamma}$		
	α (cm psi^{-1})	β	R^2	ε (% h psi^{-1})	γ	R^2
10	3.	0.6	0.9992	14.9	−1.7	0.9874
15	3.5	0.6	0.9939	–	–	–
20	–	–	–	12.1	−1.6	0.9814
25	5.8	0.4	0.9767	4.1	−1.4	0.9895

Notes: f_{th} is theoretical infiltration rate (cm h^{-1}), P is air pressure dropping rate (in psi h^{-1}), R^2 is correlation coefficient (dimensionless), α is air diffusion coefficient relying the depth of air movement into the ground per unit of pressure (in cm psi^{-1}), β is diffusion index relying the size and number of capillaries through which air moves from the surface to subsurface land (dimensionless), ε is soil-air matrix potential coefficient relying the continuous-time to saturate air into the ground per unit of pressure (in % h psi^{-1}), and γ is air-filled porosity index related to capillary potential and relative conductivity (dimensionless), θ_{th} is theoretical soil moisture content (in %).

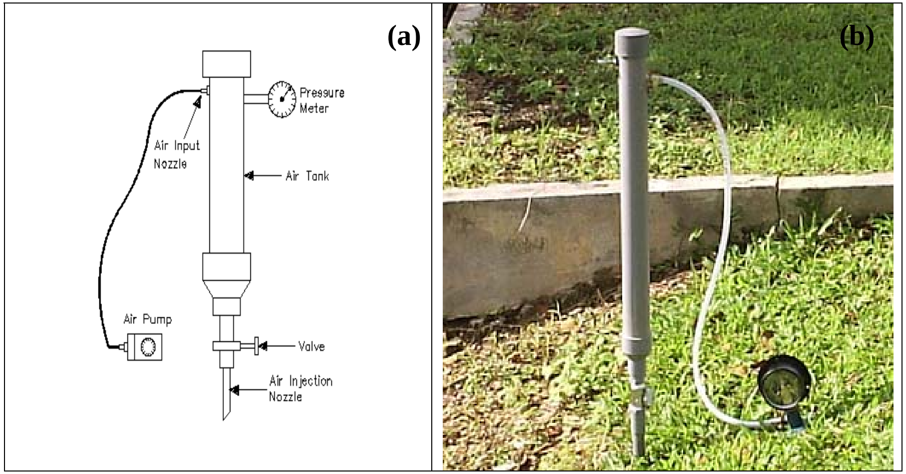

Fig. 1. Image of the aero-infiltrometer for **(a)** schematic and **(b)** physical model.

HESSD
10, 12717–12751, 2013

A new technique using the aero-infiltrometer

M. A. Fulazzaky et al.

Title Page
Abstract | Introduction
Conclusions | References
Tables | Figures
◀| |▶
◀ ▶
Back | Close
Full Screen / Esc
Printer-friendly Version
Interactive Discussion

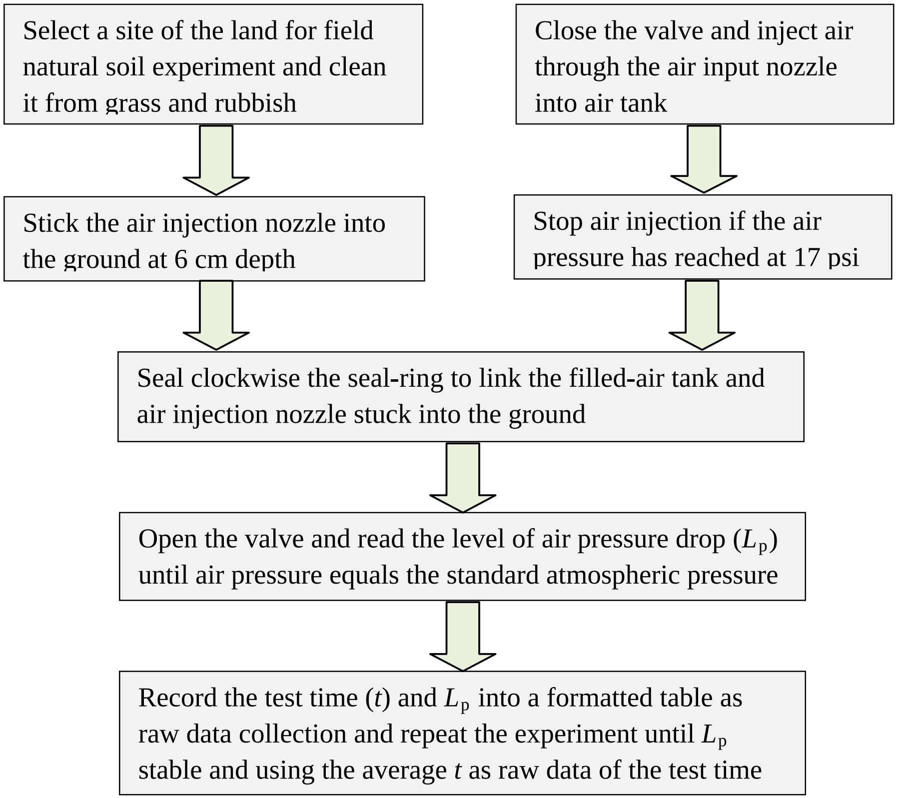

Fig. 2. Flowchart of the measurement of air diffusion into the ground by aero-infiltrometer.

HESSD
10, 12717–12751, 2013

Title Page
Abstract | Introduction
Conclusions | References
Tables | Figures
◀| |▶
◀ ▶
Back | Close
Full Screen / Esc
Printer-friendly Version
Interactive Discussion

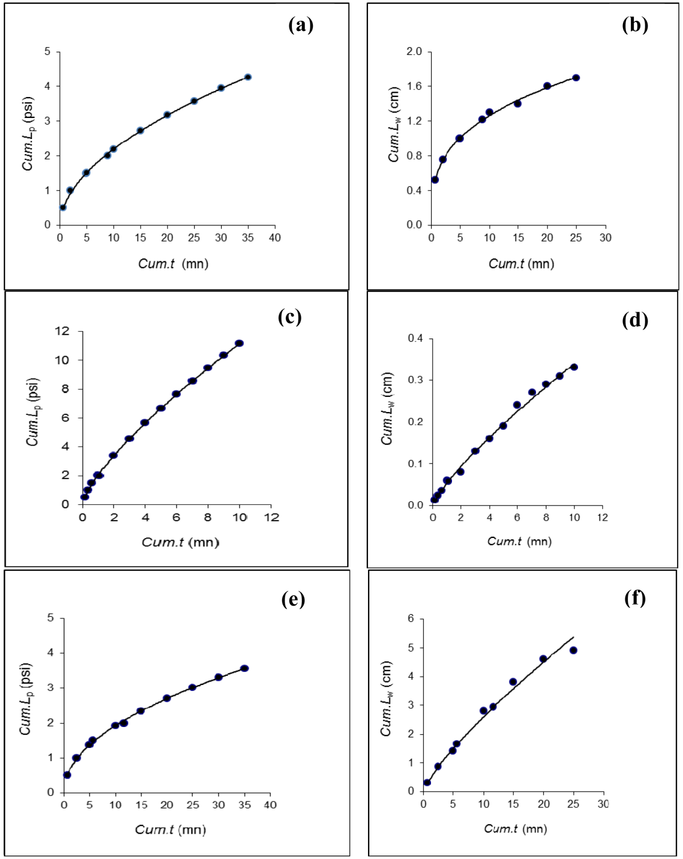

Fig. 3. Calibration of Cum.L_p using the curves of Cum.L_p vs. Cum.t; **(a)** site-1 with R^2 = 0.9984, **(c)** site-2 with R^2 = 0.9981 and **(e)** site-3 with R^2 = 0.9991 and calibration of Cum.L_w using the curves of Cum.L_w vs. Cum.t; **(b)** site-1 with R^2 = 0.9984, **(d)** site-2 with R^2 = 0.9967 and **(f)** site-3 with R^2 = 0.9966, where the correlations are evaluated through power regression analysis.

HESSD
10, 12717–12751, 2013

Title Page
Abstract | Introduction
Conclusions | References
Tables | Figures
◀| |▶
◀ ▶
Back | Close
Full Screen / Esc
Printer-friendly Version
Interactive Discussion

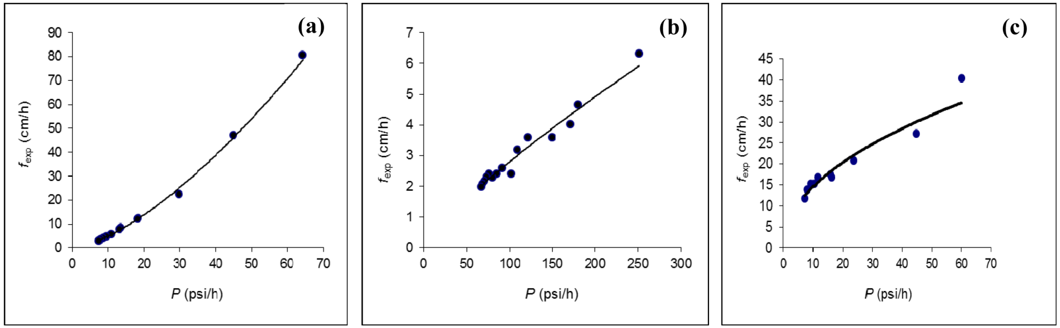

Fig. 4. Curve $f_{th} = \alpha \times P^{\beta}$; **(a)** site-1, **(b)** site-2 and **(c)** site-3.

HESSD
10, 12717–12751, 2013

A new technique using the aero-infiltrometer

M. A. Fulazzaky et al.

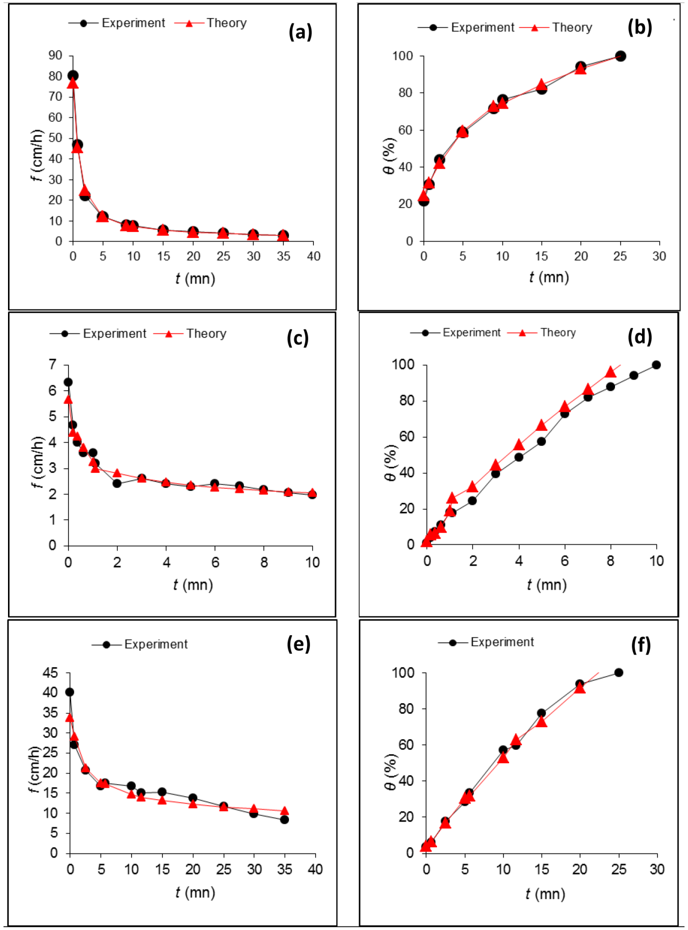

Fig. 5. Variations of f_{exp} and f_{th} pursuant to t; **(a)** site-1, **(c)** site-2 and **(e)** site-3 and variations of θ_{exp} and θ_{th} pursuant to t; **(b)** site-1, **(d)** site-2 and **(f)** site-3.

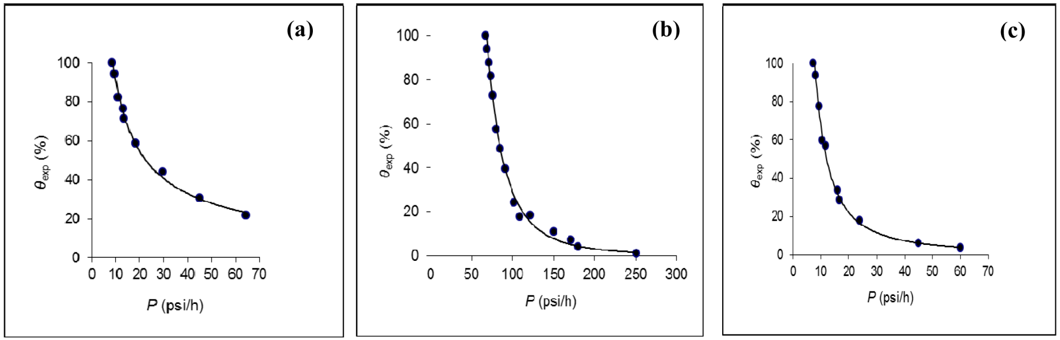

Fig. 6. Curve $\theta_{th} = \varepsilon \times P^{\gamma}$; **(a)** site-1, **(b)** site-2 and **(c)** site-3.

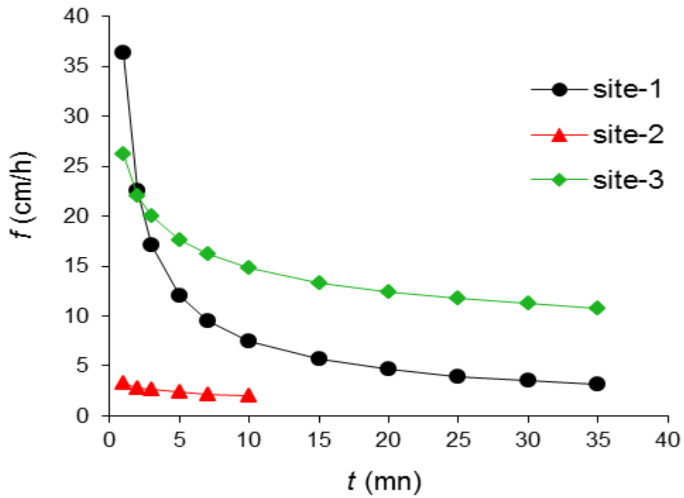

Fig. 7. Infiltration rate model of the natural soils.

HESSD
10, 12717–12751, 2013

A new technique using the aero-infiltrometer

M. A. Fulazzaky et al.

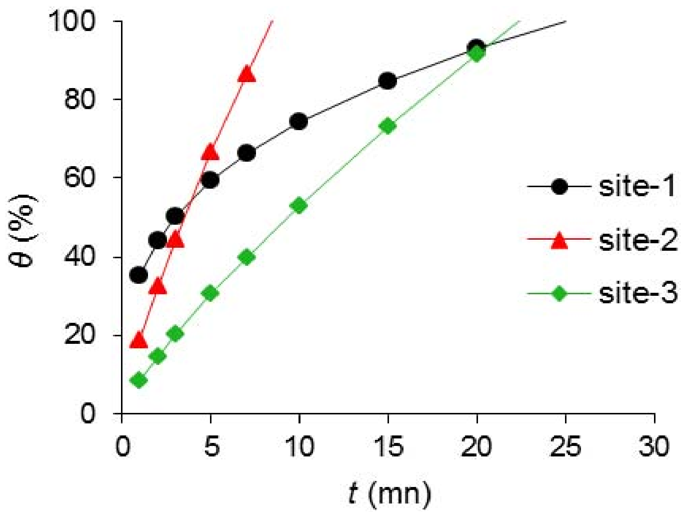

Fig. 8. Soil moisture model of the natural soils.

HESSD

10, 12717–12751, 2013

A new technique using the aero-infiltrometer

M. A. Fulazzaky et al.